[7] Simulation of characteristics of the nanophotonic electrooptical modulator on silicon-on-insulator structure

Masalsky N.V.
Scientific Research Institute for System Analysis of the Russian Academy of Sciences

Abstract

Perspective approach of simulation of the silicon nanophotonic modulator characteristics executed on the basis of silicon-on-insulator standard technical process is discussed. Optical characteristics of the waveguide structure are changed by means of effect of free carrier dispersion. On the basis of numerical calculations the device topological parameters are optimized for achievement of high modulation characteristics.

Keywords: *silicon photonic, waveguide optical structure, eloctrooptical modulator, silicon on insulator*

Citation: *Masalsky N.V. Simulation of characteristics of a nanophotonic electrooptical modulator on a silicon on insulator structure / Masalsky N.V. // Computer Optics. – 2015. – Vol. 39(2). – P. 152-157.*

Introduction

Silicon photonics now rapidly develops mostly due to recent technological and experimental achievements in the field of optical data processing [1]. Increase of integration degree in integrated optical systems (IOS) is the main direction for development of current silicon photonics [2,3]. Prerequisite for solving this problem is to develop new-generation nanophotonic devices.

Active waveguide devices (modulators and switches) which can provide excellent optical beam steering characteristics to process information are widely used in integrated optical systems (IOS). As known, general modulation methods for silicon devices are based either on thermooptical or electrooptical effects. Change of the real optical silicon refractive index is large enough due to thermooptical effect [4]. However, thermooptical effect is rather slow and it can be used for modulation frequencies within the range up to 1 MHz. For higher modulation frequencies, up to several hundred megahertz, electrooptical devices are required. In stress-free pure crystalline silicon there is no linear electrooptial effect (Pockels effect), and due to nonlinear effects, i.e. Franz-Keldysh and Kerr effects, the refractive index changes very insignificantly. Therefore, modulation methods are based on effect of free carrier dispersion [5], as a result of which both the real refractive index and the absorption coefficient of optical range radiation vary.

Concentration of free carriers in electrooptical devices can be obtained in various ways [2,6]. For this purpose, p-i-n diodes or the metal-oxide-semiconductor technology (MOS-structures) can be used.

Application of MOS-devices is characterized by high-speed performance and low power consumption. However, significant changes in concentration are possible for depletion or accumulation only in small areas (several dozens of nanometers) below area of an insulated gate. It may lead to insignificant overlap between an optical mode and non-equilibrium charge distribution in the waveguide resulting in little change of the effective refractive index. On the contrary, in pin-configuration the carriers may be injected in a larger area (the waveguide's internal region) in order to maximize the aforementioned overlap, thus increasing effective change of the refractive index. In this case, when developing the device, it should be taken into consideration that highly doped p– and n-regions should neither significantly affect the optical confinement, nor provide excessive losses. Furthermore, electric power required to change the refractive index should be low, and its level would minimize thermo-optical effect.

The main feature of the silicon-on-insulator technical process is that it can show high opportunities for production of commercially-available integrated optical systems and optoelectronic devices [2]. One of the undeniable advantages of this technology is its full compatibility with the widely used complementary metal-oxide-semiconductor technology (CMOS) [6, 7]. A silicon-on-insulator substrate has high-priority importance for integrated optoelectronic circuits with

high scale opportunities for integration of optical and electronic functions in a monocrystalline chip.

Joint usage of these two processes provides possibility to implement high-efficient optical modulation. Despite the fact that by now several types of the waveguide pin silicon-on-insulator modulators have been developed and patented in the world [2,4,6,8,9], none of them has sufficient opportunities to be applied in all possible applications. It happens mainly due to large weight-size characteristics and high power consumption. Scaling of modulator's sizes can be a promising solution here. Scaling is a very meaningful operation. It enables to improve the modulation efficiency due to greater localization of optical power, to reduce power consumption by reducing sizes of the device and to raise the modulation frequency. On the basis of computer simulation we have explored in this paper the ways of scaling the nanophotonic waveguide pin modulators which will potentially allow us to implement highly-efficient optical modulation.

1. Modulator structure

Fig. 1 shows a schematic cross-section of the analyzed silicon-on-insulator pin-configuration of the waveguide modulator. Its waveguide part is a ridge waveguide (1) located (displaced) on a thick layer of submerged silicon oxide SiO_2 (2). The height of the ridge waveguide H, the height of its ridge h_r and the base height h_s are subject to the following terms: $H=h_r+h_s$ и $h_r>>h_s$. At the base of the ridge waveguide, as regard to each lateral ridge edge, the p+ and n+ highly-doped regions (4) have been formed with impurity concentration of $1x10^{19}$ cm^{-3} and more. The width of doped regions and their distances up to lateral ridge edges have been denoted as w_d and w_s, respectively. The width of the waveguide structure is $W_w= w_r+2w_s$, where w_r – is the ridge width, whereas the total modulator width is $W=w_r+2(w_d + w_s)$. The central part of the waveguide structure (the ridge and a part of the base) is doped by n-typed impurity with basic concentration. Complete internal reflection is provided with submerged oxide and SiO_2 cladding layer which covers the whole structure.

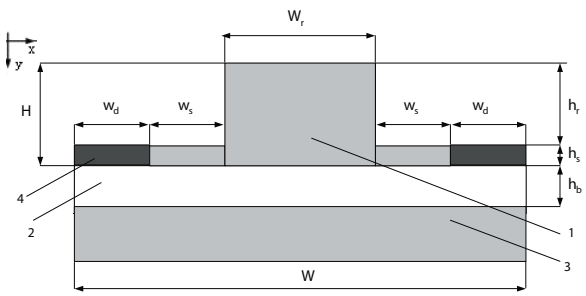

Fig. 1. Cross-section of the silicon-on-insulator pin-structure of the waveguide optical modulator, where 1 – means the silicon ridge waveguide, 2 – means SiO_2 submerged oxide, 3 – means the substrate, and 4 – means highly-doped regions

2. Generalized modulator model

For the purpose of simulation of photonic modulator characteristics it is necessary to have a common solution of the Poisson equations and the continuity equation for electrons and holes which control charge transportation in a semiconductor part of the device, and, on the other hand, of the Maxwell equation for the ridge waveguide which describes optical beam distribution therethrough.

2.1. Electric model

The commercially available 2-Dimensional simulation package ATLAS developed by SILVACO International [10] was used to calculate carriers distribution in the waveguide area. Applicability of this software package for device simulation to analyze electro-optical modulators on silicon-on-insulator waveguides was demonstrated by other authors [see, for example, 6, 11]. This software can physically simulate characteristics of semiconductor devices thus numerically solving the Poisson equations and the continuity equations for electrons and holes. The software enables to implement a complete statistical approach (Fermi-Dirac statistics), when considered, for example, highly-doped regions. Carrier recombination models include the Shockley-Read-Hall recombination (ShRH), as well as the Auge recombination and the surface recombination. The simulation package also includes thermal simulation including ohmic heat, heating and cooling due to carrier generation and recombination, the ambient temperature and the certain heat removal of the structure.

2.2. Optical model

In order to compute distribution of optical fields in the waveguide structure and optical losses due to carrier absorption we have used the beam propagation method (BMP) implemented in commercial software BeamPROP [12]. Based on concentration values for electrons and holes in any point of the pin-structure (computed by means of the electric model) we can compute the change of the real refractive index (Δn) and radiation absorption of the optical range ($\Delta\alpha$) to be determined by means of free carrier dispersion injected from highly-doped regions [5].

3. Simulation results

3.1. Initial process parameters

For characteristics simulation we have applied physical and topological parameters common to silicon electro-optical modulators [13], which are given in the table below.

Table. Parameters of the silicon-on-insulator pin-structure of the waveguide optical modulator

Parameters	Values
Optical wavelength in vacuum, nm	1552
Temperature, K	298
Silicon refractive index	3.47
SiO_2 silicon oxide refractive index	1.44
Basic level of silicon doping, cm^{-3}	$1x10^{15}$
Waveguide height, nm	210
Ridge width, nm	300
Submerged layer width, nm	940
Silicon thermal conductivity, W (see K)$^{-1}$	1.55
Silicon thermal capacity, Jcm^3	1.67

In our computations we used a carrier concentration model with regard to the Shockley-Read-Hall recombination with a supposed carrier lifetime in the central part of electrons and holes t_n=700 nc and t_p=300 nc, respectively, at basic doping concentration. It was expected while simulating that ohmic contacts are ideal. They don't introduce any additional contact resistance or capacity. Besides, electrical contacts (electrodes) are supposed to operate also as thermal contacts (heat removals) at temperature 298 K fixed.

3.2. Instrumental characteristics

The waveguide structure given in Fig. 1 maintains only one mode (a single-mode system) either for TE or for TM modes for different base thicknesses h_s. The overlap integral of optical fields of the ribbon waveguide and the waveguide ridge identifies how the change of field distribution in the ribbon waveguide can affect the total field distribution in the whole waveguide structure. The dependence of the overlap integral on the base thicknesses h_s is shown in Fig. 2.

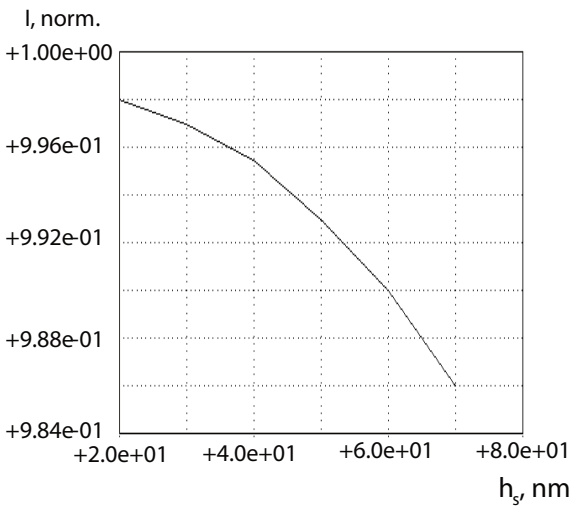

Fig. 2. The dependence of the overlap integral of ridge- and base optical fields on the base thickness

It should be noted that the overlap integral value does not practically dependent on the parameter h_s, that allows us to affirm that the use of a thin base doesn't influence on the mode distribution in the ridge of the waveguide structure if compared to the ribbon waveguide. This is important since it becomes possible to implement highly efficient interrelationship between the ridge waveguide and optical fiber.

The consumed power is one of the key parameters for this type of devices. On the one hand, it is necessary to provide high injection conditions [11], on the other hand, it is required to minimize the influence of thermo-optical effect. The simulation results show that the required injection conditions are provided at the forward bias within the range between 0.8 and 1.1 V. In this case the concentration of injected electrons and holes are practically equal in the waveguide internal region and their distributions are the same. If the forward bias potential is 0.82 V, the carriers concentration is approximately 3.3×10^{17} cm^{-3} that causes the true change of the refractive index $\Delta n = -1.1\times10^{-3}$.

The velocity of surface carrier recombination on the interface surface between the silicon waveguide and surrounding SiO_2 is one of the main factors limiting modulation characteristics of the devices. For these conditions we have shown in Fig. 3 the dependence between specific consumed statistical power and the recombination velocity.

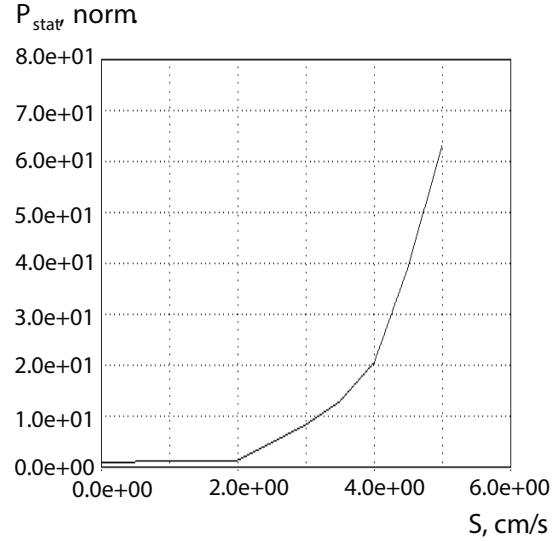

Fig. 3. The standardized dependence of specific consumed static power on the surface recombination velocity (at logarithmic scale).

Thus, for Sn=Sp=10^5 cm/sec (where Sn, Sp – is the surface recombination velocity of electrons and holes,

respectively), i.e. for the case when surface stabilizing is missing, the consumed power will sharply increase in comparison with the ideal case. This also results in considerable reduction of the concentration of injected carriers.

For the recombination velocity 10^2 cm/sec which corresponds to the case with the waveguide surface stabilized with thermally grown oxide SiO_2 [14], at the forward bias 0.82 V the specific consumed power will increase only 1.3 times with respect to the ideal case. This in turn results in slight increase of the device temperature, less than 10^{-2} K.

One of the main mechanisms for optical losses is the overlap of highly doped absorbing regions with the waveguide optical mode. It is therefore necessary to optimize the distance w_s from highly doped regions to the lateral edges of the waveguide ridge. On the one hand, the value of the parameter w_s should be large enough to reduce the overlap of these too highly absorbing regions with the optical waveguide mode. On the other hand, it should be short enough to minimize the power consumption and switch time. Similarly, the base thickness h_s must be thin enough to provide high lateral optical confinement and to reduce the overlap of highly doped regions with the optical field, but thick enough to facilitate its practical implementation. Fig. 4 shows the simulation results of the dependence of optical losses due to carrier absorption as the function w_s for different values h_s. Moreover, for the above selected conditions in ON-mode (carriers injection) the change of the absorption coefficient is $\Delta\alpha = 4.35$ см$^{-1}$.

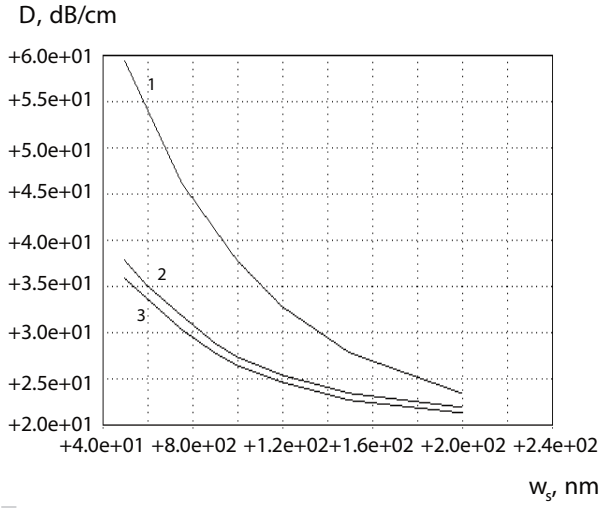

Fig. 4. The dependence of optical losses on the distance between the ridge edge and the edge of the highly doped region at different values of h_s , where 1 – h_s = 50 nm, 2 – h_s = 30 nm , 3 – h_s = 20 nm

It should be noted that losses are high for w_s<50 nm (37–59 dB/cm) within the whole range of considered values h_s. It is caused by the fact that the proximity of high doped (strongly absorbing) regions to the edge increases the overlap with the optical mode. On the other hand, losses are considerably lower when doped regions (the distance) are moved away from the lateral ridge edge. For example, when w_s=200 nm, the losses are estimated at 22–23 dB/cm in ON-mode. The results shown in Fig. 4 also illustrate that the losses increase with the increase of h_s for the given value w_s. This happens due to the fact that the thicker the base, the most part of the optical field is superimposed on highly doped regions thus increasing losses. In all cases we can observe an outstanding increment of optical losses when injecting carriers. This increase grows with a rise of the parameter h_s resulting in a greater absorption area of injected carriers. In OFF-mode (not injected carriers) the loss value is lower approximately by 20 dB / cm.

The obtained results show that from the optical point of view the base thickness must be less than or equal to 30 nm. In practical implementation the base thickness can be precisely controlled using a thermal oxidation process after the ridge etching. Thermal oxidation is also desirable to reduce the surface roughness [14].

As noted in [15], the effect of the electrode contact resistance to the total power capacity is insignificant if the contact metallization has been properly performed. For example, if the contacts Co/Si are performed on both electrodes, the respective values of contact resistance are 1.6×10^{-7} ohm×cm² and 8.9×10^{-7} ohm×cm² in highly doped n– and p-regions, respectively.

The modulator switch time from one state to another is determined by processes of either carrier diffusion or carrier removal from the internal region of the waveguide structure. In order to change the refractive index let us suppose that the switch-on time (t_{ON}) is the time required to change it from 10% to 90% of its maximum absolute value Δn. Similarly, the turn-off time (t_{OFF}) has been defined as the time required to change it from 90% to 10% of its maximum absolute value. For modeling case of the structure with h_s =20 nm and w_s=100 nm, for the switching voltage impulse into ON-state with the parameters U_{OFF}=-1 V and U_{ON}=0.82 V, the values t_{ON} and t_{OFF} shall amount to 0.84 and 0.14 ns. The total time is less than 1 ns.

Increase of the device temperature occurs during the transition from ON-state to OFF-state due to significant increase of transient reverse current. The maximum rise in temperature is 0.12 K. It is executed with one throw (by sharp upsurge and smooth decline

practically to the initial level) within the time interval just over 1 ns. It shows the effective heat removal through thermal contacts and slight thermo-optical effect.

Another simulation result has been obtained when studying the possibility to implement waveguide structures with a small curvature radius (a few microns) with no significant increase of the losses level. It is important to improve integration in integrated optical systems. For example, if the waveguide structure is curved to the left, the optical field shall be curved to the right side (+x-axis in Fig. 1) due to incurvating effect, thus considerably overlaying the doped region situated on the other side of the curvature (n+ region). Curvature-based losses become significant when the base thickness h_s increased. This is due to the fact that the higher the base, the deeper the lateral penetration of the optical field into a convex (outer) side of the curve, thus increasing the overlap with highly absorbing regions. It should be noted that the dependence of losses on w_s for the given value of the parameter h_s is similar to the aforementioned case. However, the simulation shows a remarkable property of curved structures, i.e. when the values of h_s equal to or less than 30 nm, the losses level is almost unchanged with regard to the case of the linear waveguide structure.

Conclusion

We have offered the characteristic scaling method for the nanophotonic p-i-n modulator on the silicon-on-insulator structure. Based on numerical solutions we have studied its characteristics and ways for their optimization. The simulation results show that scaling of topological sizes of the ridge waveguide can significantly reduce power consumption and provide the total switch time of less than 1 ns at acceptable optical losses and slight thermo-optical effect. For the selected configuration of the waveguide with overall dimensions of 210 nm in height and 500 nm in width, 20 nm in base height and 100 nm in distance from highly doped regions up to the ridge, for the impulse switch of controlling voltage of –1 V and 0.82 V, the switch time is less than 1 ns and power consumption is 1.45 W/m. These characteristics make the analyzed configuration very promising for the implementation of active elements based on the silicon-on-insulator nanoscale waveguide structures, and they must represent a significant step in the development of integrated optical systems with a higher degree of integration and lower power consumption.

References

1. Soifer, V.A. Nanophotonic and diffraction optics / V.A. Soifer // Computer Optics. – 2008. – Vol. 32(2). – P. 110-119. (In Russian).

2. Soref, R. The past, present, and future of silicon photonics / R. Soref // IEEE Selected Topics in Quantum Electronics. – 2006. – Vol. 12(11). – P. 1678–1687.

3. Ahn, J. Devices and architectures for photonic chip-scale integration / J. Ahn, M. Fiorentino, R.G. Beausoleil, N. Binkert, A. Davis, D. Fattal, N.P. Jouppi, M. McLaren, C.M. Santori, R.S. Schreiber, S. M. Spillane, D. Vantrease, Q. Xu // Applied Physics A. – 2009. – Vol. 95(5). – P. 989-997.

4. Cocorullo, C. Silicon thermo-optical micro-modulator with 700 kHz and 3 dB bandwidth / C. Cocorullo, M. Iodice, I. Rendina, P. M. Sarro // IEEE Photonic Technology Letters. – 1995. – Vol. 7(1). – P. 363–365.

5. Soref, R. Electro optical effects in silicon / R. Soref, B. Bennett // IEEE Quantum Electronics. – 1987. – Vol. 23(1). – P. 123-129.

6. Salib, M. Silicon Photonics / M. Salib, L. Liao, R. Jones, M. Morse, A. Liu, D. Samara-Rubio, D. Alduino, M. Paniccia // Intel Technology Journal. – 2004. – Vol. 8(1) – P. 143-160.

7. Bogaerts, W. Nanophotonic waveguides in silicon-on-insulator fabricated with CMOS technology / W. Bogaerts, R. Baets, P. Dumon, V. Wiaux, S. Beckx, D. Taillaert, B. Luyssaert, J. Campenhout, P. Bienstman, D. Thourhout // IEEE Lightwave Technology. – 2005. – Vol. 23(2). – P. 401-412.

8. Liu, A. High-speed optical modulation based on carrier depletion in a silicon waveguide / A. Liu, L. Liao, D. Rubin, H. Nguyen, B. Ciftcioglu, Y. Chetrit, N. Izhaky, M. Paniccia // Optics Express. – 2007. – Vol. 15(3).– P. 660–668.

9. Feng, N. 30GHz Ge electro-absorption modulator integrated with 3μm silicon-on-insulator waveguide / N. Feng, D. Feng, S. Liao, X. Wang, P. Dong, H. Liang, C. Kung, W. Qian, J. Fong, R. Shafiiha, Y. Luo, J. Cunningham, A. Krishnamoorthy, M. Asghari // Optics Express. – 2011. – Vol. 19(22). – P. 7062–7067.

10. Silvaco Internationnal, 4701 Patrick Henry drive, Bldg 1, Santa Clara, CA 94054 {Electronic resource]. URL: http://www.silvaco.com (request data 1.12.2012).

11. Hewitt, P.D. Improved modulation performance of a silicon p-i-n device by trench isolation / P.D. Hewitt, G.T. Reed // IEEE Lightwave Technology. – 2001. – Vol. 19(2). – P. 387-395.

12. Rsoft Photonic CAD Suite by RSoft Design Group, Inc. [Electronic resource]. URL: http://www.rsoftdesign.com (request data 27.01.2014).

13. Masalsky, N.V. Characteristics of the submicronic photon phase modulator on structure “silicon on an insulator” / N.V. Masalsky // Nano and microsystem technique. – 2013. – Vol. – P. 38-42. (in Russian).

14. Cutolo, A. Silicon electro-optic modulator based on a three terminal device integrated in a low-loss single-mode SOI waveguide / A. Cutolo, M. Iodice, P. Spirito, L. Zeni // IEEE Lightwave Technology. – 1997. – Vol. 15(2). – P. 505-511.

15. Nakatsuka, O. Contact resistivities and electrical characteristics of Co/Si contact by rapid thermal annealing / O. Nakatsuka, T. Ashizawa, H. Iwano, S. Zaima, Y. Yasuda // in Proc. Adv. Metallization Conf. (AMC 1998) . – 1999. – Vol. 784. – Warrendale, PA. – P. 605–610.